Composition Distributions of Different Particles of a Polypropylene/Poly(ethylene-*co*-propylene) *In Situ* Alloy Analyzed by Temperature-Rising Elution Fractionation

Jun-Ting Xu, Wei Jin, Zhi-Sheng Fu, Zhi-Qiang Fan

Department of Polymer Science and Engineering, Zhejiang University, Hangzhou 310027, People's Republic of China

Received 6 April 2004; accepted 6 February 2005
DOI 10.1002/app.22085
Published online in Wiley InterScience (www.interscience.wiley.com).

ABSTRACT: Fragmentation was observed in the polymerization process for the preparation of a polypropylene (PP)/poly(ethylene-*co*-propylene) (EPR) *in situ* alloy. Composition distributions of different polymer particles were analyzed by preparative temperature-rising elution fractionation. The fractions eluted at room temperature and 96, 110, and 117°C were selected for ^{13}C-NMR characterization. There was more propylene homopolymer and ethylene–propylene block copolymer in the large particles, whereas the small particles contained more ethylene–propylene random copolymer and copolymer with a transition microstructure. On the basis of the formation mechanism of various components in the PP/EPR alloy, we inferred that the fragmentation of the polymer particles mainly took place in the copolymerization step. © 2005 Wiley Periodicals, Inc. J Appl Polym Sci 98: 243–246, 2005

Key words: fractionation of polymers; poly(propylene) (PP); alloys

INTRODUCTION

The polypropylene (PP)/poly(ethylene-co-propylene) (EPR) *in situ* alloy is one type of polyolefin with high performance. It has a good balance between tensile and impact mechanical properties and can be used to replace parts of engineering plastics. The PP/EPR *in situ* alloy is usually prepared through three steps.[1–3] In the first step, the prepolymerization of propylene is conducted to yield high polymerization activity and to maintain the morphology of the catalyst. The homopolymerization of propylene and the copolymerization of propylene with ethylene are carried out in the second and third steps, respectively. Because of the nonliving nature of coordination polymerization, the PP/EPR *in situ* alloy has a complicated microstructure. Ethylene–propylene block copolymer, ethylene–propylene random copolymer, and propylene homopolymer can coexist in the PP/EPR *in situ* alloy.[4–10] The microstructure of the PP/EPR *in situ* alloy, for example, the weight percentage of various components and the composition of the components, has a great influence on its ultimate application and processing properties.[11–14] Apart from its microstructure, another important aspect is the morphology of the polymer particles during polymerization. When polymerization is well controlled, the polymer particles will copy the spherical morphology of the catalyst. In the second step, the propylene homopolymer should form a hollow shell, and in the third step, the copolymerization of ethylene with propylene occurs inside the shell so that the polymer particles will not stick to the wall of the reactor, despite the presence of copolymers with low melting temperatures. The core–shell structure is also advantageous to the mechanical properties of the PP/EPR *in situ* alloy. Nevertheless, we found that in the practical polymerization process, the fragmentation of the polymer particles always takes place to greater or lesser extent. In this study, the microstructures of different polymer particles were analyzed with preparative temperature-rising elution fractionation (TREF) and NMR. This study helped us to understand the structural differences among the different polymer particles and to evaluate the effect of fragmentized particles on the properties of the PP/EPR *in situ* alloy.

EXPERIMENTAL

Preparation of the PP/EPR alloy

The PP/polyethylene (PE) alloy was prepared through three polymerization steps. About 270 g of purified liquid propylene was added into an autoclave, in which 30 mg of $MgCl_2$-supported $TiCl_4$ catalysts (type JLH22-3, donated by Beijing Research Institute of Petrochemical Technology), external donor

Correspondence to: J.-T. Xu (xujt@zju.edu.cn).
Contract grant sponsor: Special Funds for Major State Basic Research Projects; contract grant number: G1999064803.

(dicyclohexyl dimethoxysilane/Ti = 20), and cocatalyst ($AlEt_3$/Ti = 250) were pre-added. The propylene prepolymerization was first carried out for 30 min at 20°C. Then temperature was raised to 70°C, and the bulk polymerization of propylene started. After bulk polymerization was performed for 1 h, the polymer particles were transferred to another reactor that was *in vacuo*. Subsequently, the propylene gas transferred together with the polymer particles was removed under reduced pressure, and the mixed gas of ethylene and propylene was introduced. The pressure of the mixed gas was 0.5 MPa, and the molar percentage of ethylene was 30%. The copolymerization of ethylene and propylene lasted for 2 h at 60°C.

Fractionation with preparative TREF

A preparative TREF apparatus was used to collect a sufficient amount of polymer fractions.[15] About 2 g of polymer was dissolved in xylene at a concentration of 0.005 g/mL at 130°C. This solution was deposited on an inert support, sea sand (particle diameter = 0.3–0.6 mm), packed in a steel column. The length and the internal diameter of the column were 1.0 m and 40 mm, respectively. The column was cooled to room temperature at a rate of 1.5°C/h. Then, the deposited polymer was heated stepwise and eluted with xylene at different temperatures. The polymer fractions were recovered by the evaporation of the xylene solvent and by drying in a vacuum oven.

^{13}C-NMR characterization

^{13}C-NMR spectra were recorded on a Bruker AMX500 NMR spectrometer (Bruker, Rheinstetten, Germany) at 120°C with hexamethyldisiloxane as the internal standard. The solutions were prepared in *o*-dichlorobenzene-d_4 at a concentration of 0.1 g/cm^3. The number of scans was 3000, and the delay time was 10 s.

TABLE I
TREF Data for the Overall Sample

Elution temperature (°C)	W_i%	ΣW_i%	W_i%/ΔT
5	13.74	13.74	—
53	3.42	17.16	0.0673
77	5.28	22.44	0.221
92	3.67	26.11	0.240
96	3.78	29.89	0.942
102	4.25	34.14	0.712
107	8.30	42.44	1.664
109	10.62	53.06	5.318
111	10.80	63.86	5.404
114	16.74	80.60	5.577
117	7.34	87.94	2.443
120	5.91	93.85	1.971
125	4.93	98.78	0.981
130	1.28	100	0.240

TABLE II
TREF Data for the Large Particles

Elution temperature (°C)	W_i%	ΣW_i%	W_i%/ΔT
8	7.23	7.23	—
59	6.61	13.84	0.134
75	2.06	15.90	0.134
89	2.06	17.96	0.156
96	3.81	21.77	0.547
102	8.28	30.05	1.384
106	8.70	38.75	2.176
109	6.57	45.32	2.187
111	12.58	57.90	6.294
114	5.58	63.48	1.864
117	17.60	81.08	5.870
120	9.03	90.11	3.013
126	7.83	97.94	1.306
130	2.06	100	0.513

RESULTS AND DISCUSSION

The TREF data of the overall sample, large particles and small particles, are summarized in Tables I–III, and the cumulative curves (ΣW_i% vs T, where ΣW_i% is the cumulative weight percentage of eluted-fractions, and T is the elution temperature) and derivative curves (W_i%/ΔT vs T, where ΔT is the difference in elution temperature of two adjacent fractions) are illustrated in Figures 1–3. When we concentrated on the regions above 100°C in the W_i%/ΔT versus T curves (where W_i% is the weight percentage of the fraction), we found that only a broad peak appeared in the overall sample, whereas this peak split into two sharp peaks, which were located at 110 and 117°C, in the large particles and small particles, respectively. The maxima of these two peaks in the small particles were

TABLE III
TREF Data for the Small Particles

Elution temperature (°C)	W_i%	ΣW_i%	W_i%/ΔT
5	25.98	25.98	—
56	13.39	39.37	0.259
77	12.04	51.41	0.575
91	8.62	60.03	0.603
96	5.54	65.57	1.121
102	4.72	70.29	0.776
107	4.34	74.63	0.862
110	4.59	79.22	1.523
114	4.29	83.51	1.063
117	5.00	88.51	1.667
120	3.27	91.78	1.092
125	3.48	95.20	0.690
130	4.80	100	0.948

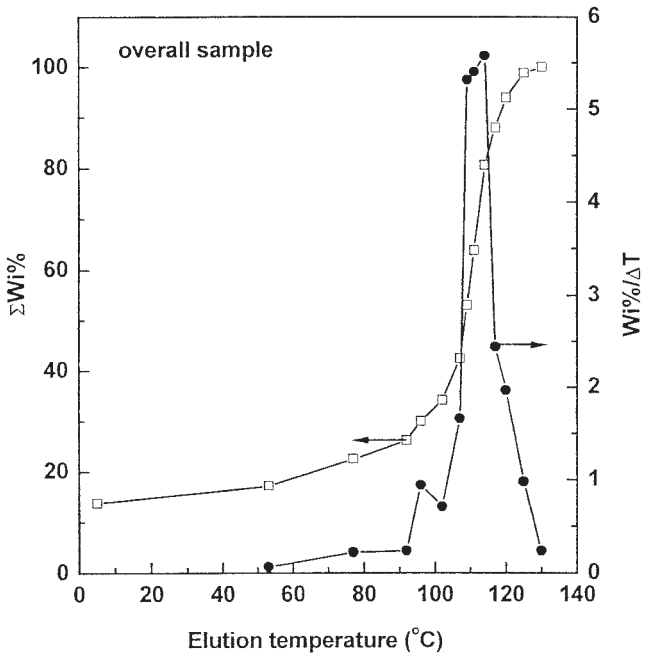

Figure 1 TREF curves of the overall sample.

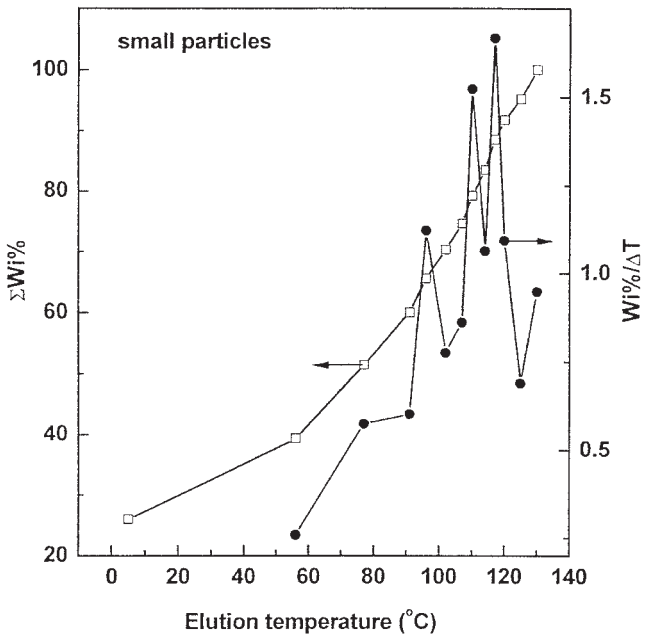

Figure 3 TREF curves of the small particles.

far lower than those in the large particles. There was a weak shoulder peak at 96°C in the overall sample that was absent in the large particles but present with high relative intensity in the small particles. When the weight percentage of the fraction eluted at room temperature in the $\Sigma W_i\%$ versus T curves was compared, we saw that the small particles had a much large room-temperature fraction than the large particles, and the overall sample had a room-temperature fraction with intermediate content. The fractionation data showed that the TREF curve of the overall sample was a combination of the TREF curves of the large particles and the small particles, as expected. The small particles contained fewer fractions eluted in the high-temperature range, but more fractions eluted in the low-temperature range.

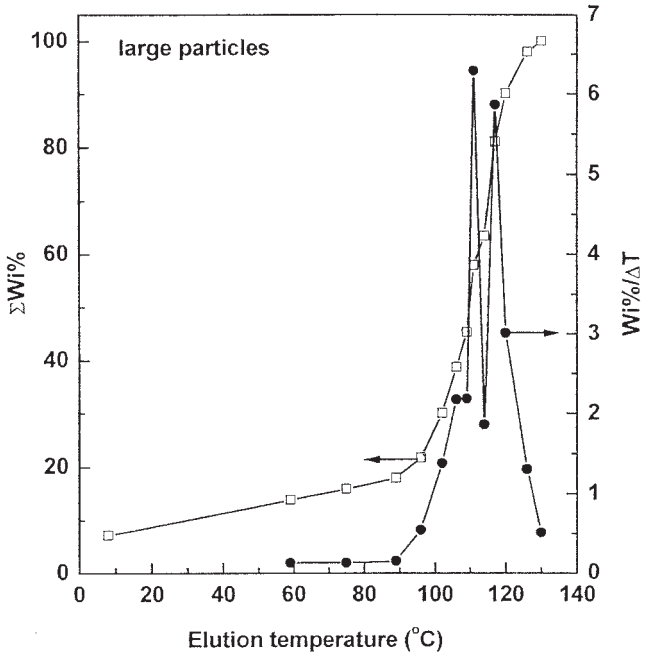

Figure 2 TREF curves of the large particles.

To understand the microstructure of fractions eluted at various temperatures, some fractions were selected for ^{13}C-NMR characterization. The triad distributions of the fractions eluted at room temperature and 96, 110, and 117°C are given in Table IV. The ^{13}C-NMR data revealed that the fraction eluted at room temperature was a random copolymer of ethylene–propylene. The fraction eluted at 117°C was the propylene homopolymer. The fraction eluted at 110°C was a multiblock copolymer of ethylene–propylene because this fraction contained both long sequences of ethylene and propylene segments, but the resonances due to the junctions of these two segments, PPE and

TABLE IV
Triad Sequence Distributions of Some Selected Fractions

Elution temperature (°C)	PPP	PPE	EPE	EEE	PEP	PEE
Room temperature	22.7	3.6	24.1	20.2	7.9	21.5
96	50.3	2.1	3.8	36.9	1.9	5.0
110	78.9	0	0.1	20.8	0	0.2
117	1000	0	0	0	0	0

PPP, PPE, EPE, EEE, PEP, and PEE are triads of monomer sequences distribution calculated from 13C NMR spectra.

PEE, were observed as well. The microstructure of the fraction that eluted at 96°C was a little more complicated. It contained not only long sequences of ethylene and propylene but also a small amount of triads such as EPE and PEP, which were attributed to random sequences. As a result, there existed some transition sequences between the long ethylene and propylene sequences in this fraction. We called this fraction the *transition copolymer* because it had a microstructure between the random copolymer and the block copolymer. The microstructures of these selected fractions were in accordance with our previous findings.[14] In combination with the TREF data and ^{13}C-NMR results, the small particles contained more random copolymer and transition copolymer but less multiblock copolymer and propylene homopolymer.

We also explained how these fractions with different microstructures were produced in terms of polymerization processing and the characteristics of plural active sites in heterogeneous Ziegler–Natta catalysts.[15,16] PP was mainly produced in the homopolymerization step by the active sites of short lifetime or the active sites with chain-transfer reactions to hydrogen. Random copolymer fractions were produced by the active sites and showed little polymerization selectivity to ethylene and propylene with chain-transfer reactions to hydrogen in the copolymerization step. The block copolymer was formed in the copolymerization step by the active sites and exhibited a high tendency toward homopolymerization for both monomers. On the basis of these analyses, we concluded that the fragmentation of polymer particles took place mainly at the copolymerization step, and the small particles were rich in newly generated active sties due to chain transfer to hydrogen.

CONCLUSIONS

The TREF data and ^{13}C-NMR results showed that the composition distribution of the large particles and the small particles of the PP/EPR *in situ* alloy were different. The large particles were rich in propylene homopolymer and ethylene–propylene block copolymer, whereas the small particles contained more ethylene–propylene random copolymer and copolymer with a transition microstructure. These findings indicate that fragmentation of the polymer particles was most likely to take place in the copolymerization step.

References

1. Simonazzi, T.; Cecchin, G.; Mazzullo, S. Prog Polym Sci 1991, 16, 303.
2. Galli, P.; Haylock, J. C. Prog Polym Sci 1991, 16, 443.
3. Galli, P. Prog Polym Sci 1994, 19, 959.
4. Fan, Z. Q.; Zhang, Y. Q.; Xu, J. T.; Wang, H. T.; Feng, L. X. Polymer 2001, 42, 5559.
5. Mirabella, F. M. J. J Polym Sci Appl Polym Symp 1992, 51, 117.
6. Mirabella, F. M. J. Polymer 1993, 34, 1729.
7. Usami, T.; Gotoh, Y.; Umemoto, H.; Takayama, S. J Polym Sci Appl Polym Symp 1993, 52, 45.
8. Zhang, X. Q.; Olley, R. H.; Huang, B. T.; Bassett, D. C. Polym Int 1997, 43, 45.
9. Xu, J. T.; Feng, L. X.; Yang, S. L.; Wu, Y. N.; Yang, Y. Q.; Kong, X. M. Polymer 1997, 38, 4381.
10. Cai, H. J.; Luo, X. L.; Ma, D. Z.; Wang, J. M.; Tan, H. S. J Appl Polym Sci 1999, 71, 93.
11. Cai, H. J.; Luo, X. L.; Chen, X. X.; Ma, D. Z.; Wang, J. M.; Tan, H. S. J Appl Polym Sci 1999, 71, 103.
12. Feng, Y.; Hay, J. N. Polymer 1998, 39, 6589.
13. Feng, Y.; Jin, X.; Hay, J. N. J Appl Polym Sci 1998, 68, 381.
14. Xu, J. T.; Feng, L. X. Polym Int 1998, 47, 433.
15. Xu, J. T.; Feng, L. X. Eur Polym J 2000, 36, 867.
16. Xu, J. T.; Fu, Z. S.; Fan, Z. Q.; Feng, L. X. Eur Polym J 2002, 38, 1739.